ELSEVIER

Contents lists available at ScienceDirect

International Journal of Biological Macromolecules

journal homepage: www.elsevier.com/locate/ijbiomac





Non-invasive characterization of the elastic protein resilin in insects using Raman spectroscopy

Charlie Woodrow^a, Darron A. Cullen^{a,c}, Fernando Montealegre-Z^a, Jose Gonzalez-Rodriguez^{b,*}

- ^a University of Lincoln, School of Life and Environmental Sciences, Joseph Banks Laboratories, Green Lane, Lincoln LN6 7DL, United Kingdom of Great Britain and Northern Ireland
- b University of Lincoln, School of Chemistry, Joseph Banks Laboratories, Green Lane, Lincoln LN6 7DL, United Kingdom of Great Britain and Northern Ireland
- c University of Hull, School of Natural Sciences, Cottingham Road, Hull, HU6 7RX, United Kingdom of Great Britain and Northern Ireland.

ARTICLE INFO

Keywords: Insect cuticle Chitin Polysaccharide Elastomers Elastic proteins

ABSTRACT

Resilin is an extremely efficient elastic protein found in the moving parts of insects. Despite many years of resilin research, we are still only just starting to understand its diversity, native structures, and functions. Understanding differences in resilin structure and diversity could lead to the development of bioinspired elastic polymers, with broad applications in materials science. Here, to better understand resilin structure, we offer a novel methodology for identifying resilin-rich regions of the insect cuticle using non-invasive Raman spectroscopy in a model species, the desert locust (*Schistocerca gregaria*). The Raman spectrum of the resilin-rich semilunar process of the hind leg was compared with that of nearby low-resilin cuticle, and reference spectra and peaks assigned for these two regions. The main peaks of resilin include two bands associated with tyrosine at 955–962 and 1141–1203 cm⁻¹ and a strong peak at 1615 cm⁻¹, attributed to the α -Amide I group associated with dityrosine. We also found the chitin skeletal modes at \sim 485–567 cm⁻¹ to be significant contributors to spectra variance between the groups. Raman spectra were also compared to results obtained by fluorescence spectroscopy, as a control technique. Principal component analysis of these resulting spectra revealed differences in the light-scattering properties of resilin-rich and resilin-poor cuticular regions, which may relate to differences in native protein structure and relative abundance.

1. Introduction

Resilin, first described in the wing joints of flying insects [1] is the most efficient elastic protein in nature [2]. Its mature structure consists of coiled peptide chains held in an isotropic 3D network by tyrosine (Tyr) and dityrosine (di-Tyr) cross-linking [3–5]. In its natural state, mature resilin is intercalated with the structural polysaccharide chitin (the tough exoskeletal material of insects), a derivative of glucose, to form a lattice with both high elasticity and high structural integrity. All moving parts of the insect exoskeleton, including wing hinges, legs, and antennal joints, apodemes (tendons), and intersegmental articulations, contain resilin-chitin composites of varying proportions.

Peptide chains resulting from the cross-linking of dityrosine and tyrosine are highly autofluorescent under UV excitation, and thus fluorescence emission is classically used to identify resilin in insect structures [5]. However, this technique does not provide quantitative or chemical information on the relative compositions of chitin and resilin

in the insect organs, or the native resilin sequence. Identifying chemical functional groups in different resilin samples, or differences in local resilin structure, is beyond the scope of traditional fluorescence techniques, but could help us to infer material properties such as elasticity, and to determine whether the folding of the resilin protein differs across species and expression sites. Such knowledge would be crucial to the rapidly advancing field of biophysical entomology, particularly in advancing theoretical and numerical modelling.

In this work, we present a non-invasive characterization of resilin and chitin in insect tissues using Raman spectroscopy, to improve previous invasive measurements of insect chitin [6] and create a Raman spectrum library for future studies of insect resilins. Raman spectroscopy, which is being increasingly used in biological studies [7], is a light scattering technique that allows for the building of a fingerprint of a molecule of interest, through unique scattering of UV, visible, or NIR light [8]. The unique scattering depends on the vibrational modes of the molecules, and thus can be used to infer compositions and native

E-mail address: jgonzalezrodriguez@lincoln.ac.uk (J. Gonzalez-Rodriguez).

^{*} Corresponding author.

structures of samples of interest.

Raman has been proven to be an effective tool for the characterization of in situ insect tissues and we here demonstrate that, in a complimentary manner to traditional fluorescence methods, resilin-rich tissues and cuticle can be identified based on differences in their Raman spectra. Furthermore, these signatures can be neatly differentiated from the collected spectra using principal component analysis (PCA). Raman shifts are identified for resilin and chitin based on non-invasive measurements in the desert locust (*Schistocerca gregaria*), and the benefits and challenges of Raman imaging of insect tissues is discussed.

2. Methodology

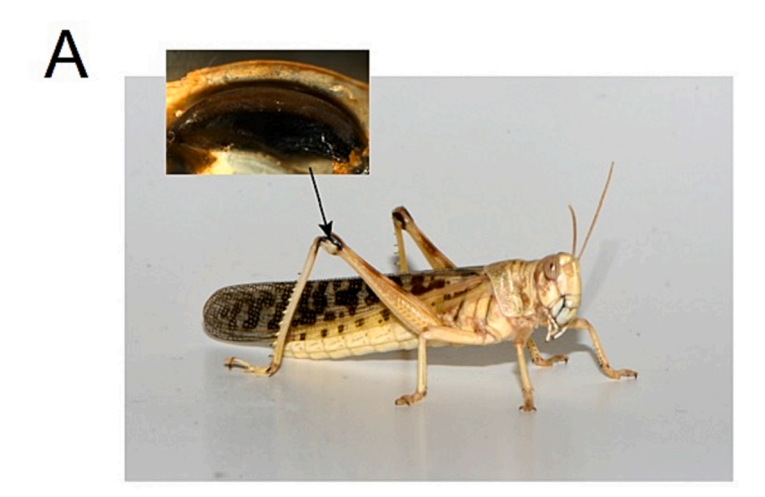
2.1. Samples and sample preparation

A well-studied resilin-containing structure is the locust semilunar process (SLP), a bow-like region of highly sclerotized cuticle situated on the hind femur at its joint with the tibia (Fig. 1A). The SLP is formed from a lattice of resilin and chitin, which together give the combination of rigidity and elastic recovery needed for energy storage prior to powerful jumping [5]. We therefore used the SLP as a structure rich in resilin. For a control region of the insect with relatively little resilin, we used the middle of the hind femur. Thus, to prepare samples, 15 hind legs were removed from euthanized desert locusts (*Schistocerca gregaria*) at colonies held at the University of Lincoln, UK. To validate the use of

Raman spectroscopy as a non-invasive method, no further sample preparation was performed, and the legs simply placed on a microscope slide to manipulate under the Raman microscope. Resilin and chitin both consist of Raman active cyclic monomers which differ in their functional groups (Fig. 1B), making them amenable to non-invasive Raman techniques. A synthetic L,L-dityrosine (Bioquote Ltd., York, UK) and powdered chitin purified from shrimp shells (Sigma-Aldrich, Inc., St. Louis, United States) were also obtained, to repeat the experiments on native compounds free from other interfering molecules.

2.2. Raman analysis

Raman analysis was performed with a Horiba Jobin Yvon Labram (HORIBA, Kyoto, Japan) coupled to an Olympus BX41 confocal microscope (Olympus Corporation, Shinjuku, Tokyo, Japan) with a laser operating at a wavelength of 532 nm. The video confocal microscope integrated into the machine permitted visualization of samples and placement of the laser beam to an appropriate position and focal depth on the sample. As the samples are not well described using Raman prior to this analysis, spectra were initially collected between wavenumbers 3500 and 200 cm⁻¹ (Rayleigh scattering). To obtain optimal settings for spectrum acquisition, samples were subjected to different acquisition times and laser intensities. Exposure times during these tests ranged from 1 s to 20 s. All spectra were averaged a minimum of 10 times during the acquisition process. The settings to obtain optimal spectra varied



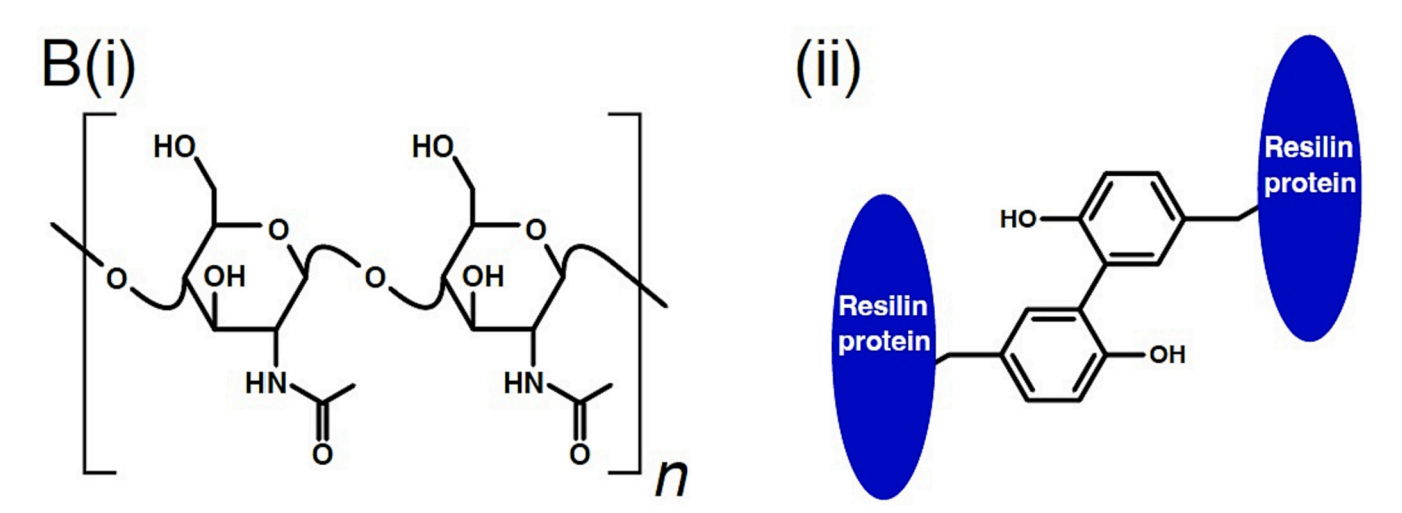


Fig. 1. (A) The desert locust, *Schistocerca gregaria*. Inset image shows a magnified view of the resilin-rich semi-lunar process of the femorotibial joint, indicated by the arrow. (B) Chemical structures of (i) chitin and (ii) dityrosine, the amino acid dimer responsible for the autofluorescence of resilin.

considerably between samples, but as suggested by previous authors investigating Raman in insect tissues, low intensities and long acquisition times provided better spectra [6]. Thus, acquisition settings of 25 % laser intensity, 12 second exposure, and 10× averaging were consequently chosen as a starting point for each sample. The slit area remained between 100 and 400 nm. Due to differences in sample orientation and data acquisition settings, Raman spectra can vary slightly between samples, however the relative intensities of peaks within the spectra will remain constant. In addition, the experiments described in the present work were performed using a confocal Raman system, allowing for a detailed description of tissue layers of different focal planes at a micrometer level [9]. Therefore, we can use ratios of different peaks to further compare samples, irrespective of acquisition protocols, as long as the user is confident in the laser position in the confocal plane. To demonstrate the utility of this technique for insect samples, a cuticle sample from the specimen of interest was placed on top of a sample of naphthalene, which has a well-characterized Raman spectrum. As shown in Supplemental Fig. 1, we could not only identify the Raman spectrum from the outer cuticle, but also penetrate deeper through the sample to identify the characteristic spectrum of naphthalene. This is evidence of the ability of Raman to investigate Raman active biomolecules inside the insect body. With this in mind, once the insect resilin spectra were collected and peaks identified, a principal component analysis (PCA) was performed using the wavenumbers and relative intensities of peaks which were present in both of the sample types, to discern whether there are significant differences between the two spectra. The 1st and 2nd principal components resulting from the PCA were then tested for statistical differences between the resilin-rich and low-resilin samples. This was computed using a One-way PERMANOVA with 9999 permutations in Past 4.03 [10].

2.3. Fluorescence microscopy

Although well detailed from existing studies, we used fluorescence microscopy to confirm the presence of resilin in the samples of interest. This was done using an Olympus BX51W1 compound microscope [11] fitted with a DAPI-5060B Brightline UV filter set (Semrock, Rochester,

NY, USA; excitation 350–407 nm, emission 413–483 nm). Under this filter set, resilin-rich structures display a strong blue autofluorescence. Images were taken for the locust semilunar process, the middle of the hind femur, hind leg tendon, and synthetic dityrosine. Additional amino acids (in powdered form) were imaged to compare fluorescence emission to that of dityrosine.

3. Results

3.1. Raman spectroscopy

As has been suggested previously for insect tissues [6], successful spectra were collected most frequently during low laser intensities (0.1–25 %) coupled with long exposure times (12–20 s) with moderate averaging (10 \times).

Standard examples of the Raman spectra obtained from the control region of the locust hind femur and semilunar process are shown in Fig. 2, with their peak assignments summarized in Table 1. At first observation, it is clear that there are differences in the spectra obtained from the different regions of the hind leg. At \sim 484 and \sim 567 cm⁻¹, we observe vibrations of the basic chitin skeletal mode [12,13]. These are clear in the hind femur, but less often observed in the semilunar process (Fig. 2). From here, there are few regularly occurring peaks in either sample type, until \sim 850 cm⁻¹ where a small peak is observed, often as a shoulder to the well-defined peak at \sim 955 cm⁻¹; which we assign to the amino acid tyrosine [12,14]. The peak at \sim 850 cm⁻¹ could represent the well-known tyrosine doublet [15], but discrimination of the doublet beyond this interpretation is challenging in the assessed samples. Peaks at ~1003, 1040, and 1106 cm⁻¹ are assigned to either C—C or C—N stretching modes, and are more often observed in the hind femur samples [6,16]. Between ~1141 and 1203 cm⁻¹, there are 2 prominent peaks which are substantial in the semilunar process. These peaks are attributed to C(2)-OH groups characterized by tyrosine [6,13,14,17]. At \sim 1327 and 1419 cm $^{-1}$ there are several small peaks associated to strong CH deformation. These have been attributed to chitin in other studies of insect tissues [12]. In the region of 1450 cm⁻¹, the hind femur samples show small peaks we assign to CH₂ or CH₃ deformation [12,16,17]. At

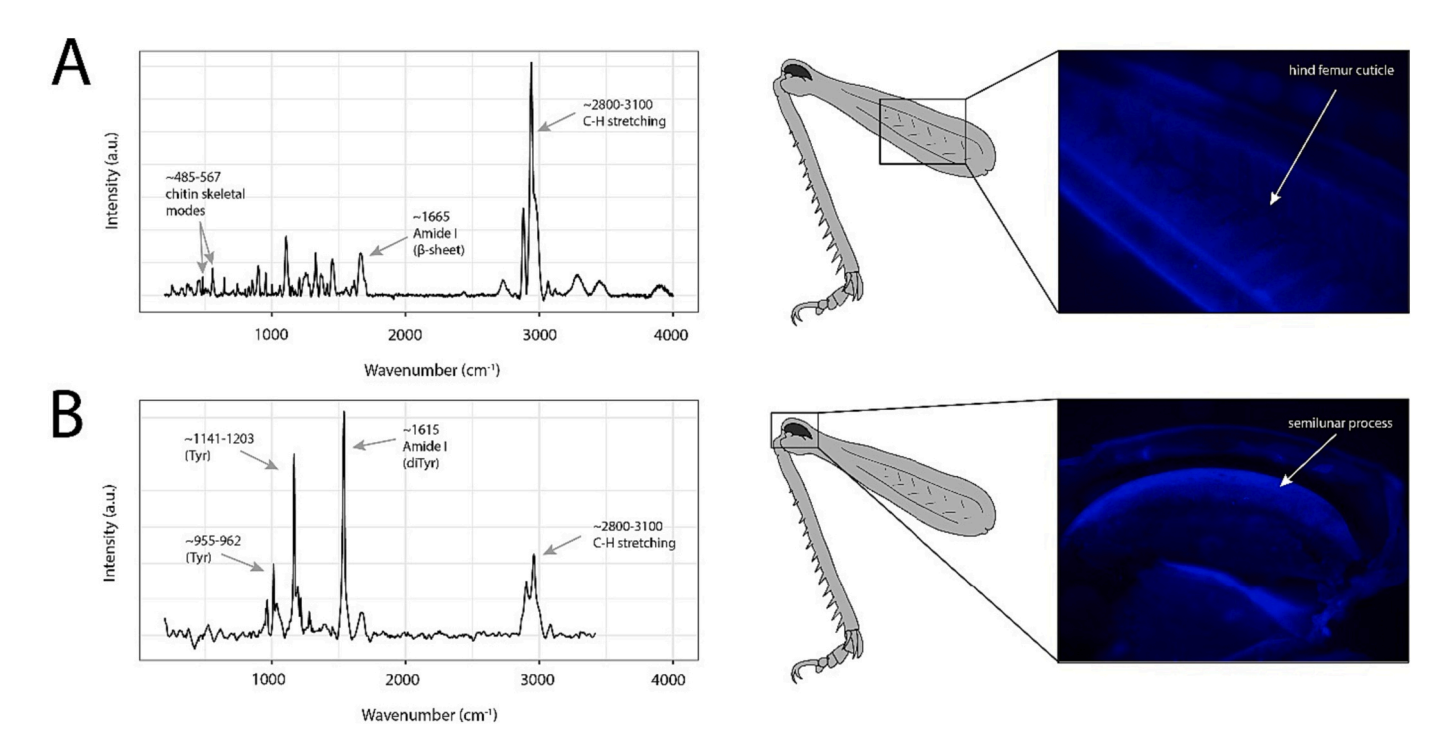


Fig. 2. Representative Raman spectra, location of collected spectra, and fluorescence microscopy for control hind leg cuticle (A) and resilin-rich semilunar process (B). Labelled peaks represent wavenumbers used in PCA for discrimination between resilin and chitin.

Table 1Library of wavenumbers and their assignments identified in this study. Assignments confirmed by supporting studies cited.

| Wavenumber (cm ⁻¹) | Assignment and notes | References |
|--------------------------------|---|--------------|
| 2800-3100 | C-H stretching | [6,16] |
| 1665 | Amide I (β-sheet), potential contributions from multiple secondary structures | [6,16–18] |
| 1615 ^a | Amide I, resilin, diTyr, comparable to synthetic proresilin AN16 | [6,14,17,18] |
| 1525 | Amide II | [13] |
| 1450 | CH ₂ /CH ₃ deformation | [12,16,17] |
| 1419 | Chitin | [12] |
| 1377 | CH deformation, chitin | [12] |
| 1327 | Chitin | [12] |
| 1265 | Amine III (β-sheet) | [6,16] |
| 1203 ^a | Resilin, Tyr | [14,17] |
| 1151 ^a | C(2)-OH, resilin, Tyr | [6,13,17] |
| 1106 | C-C stretching | [6] |
| 1040 | C-C and C-N stretching modes or Phe | [6,16] |
| 1003 | CC-stretch (β-sheet) or Phe | [16,17] |
| 955 ^a | Resilin, Tyr | [12,14] |
| 830-850 | Tyr, Fermi resonance doublet | [15] |
| 567 ^a | Chitin skeletal mode | [12,13] |
| 484 ^a | Chitin skeletal mode | [12,13] |

^a Indicates a wavenumber of interest for differentiating resilin and chitin in insect tissues.

 \sim 1615 cm⁻¹ is the largest peak in the semilunar process samples, an Amide 1 mode attributed to tyrosine/dityrosine [6,14,17,18]. At \sim 1665 cm⁻¹ signals are recorded which can be attributed to amide I (β -sheet), with potential contributions from multiple secondary structures [6,16–18]. Finally, from \sim 2800–3100 cm⁻¹, are a prominent series of peaks, often represented as a series of shoulders to a main peak at \sim 2940 cm⁻¹ which correspond to C—H stretching [6,16].

3.2. Principal component analysis (PCA)

To assist interpretation of the spectra between the semilunar process and hind femur samples, principal component analysis (PCA) was performed using the wavenumbers and relative intensities of 6 peaks which were present in both of the sample types (Fig. 3). The 6 peaks chosen for PCA are labelled in Fig. 2 and indicated in Table 1 with an *. The PCA reveals that the two sample types cluster differently and can thus be distinguished based on these 6 peaks alone. Variations in the PC scores for individual samples are down to small variations in relative intensities of the peaks. PC scores for the two-dimensional axes account for 95.62 % (X = 59.77 %, Y = 35.85 %) of variation between the datapoints.

PCA revealed that the first two principal components explained a

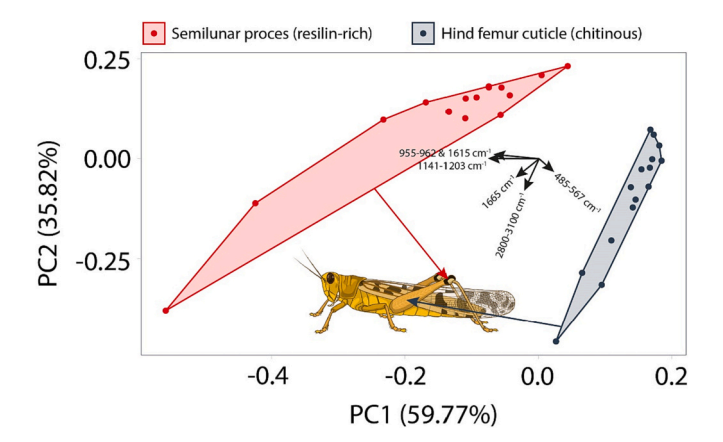


Fig. 3. Principal component analysis of the Raman spectra from the locust semilunar process and hind femur control cuticle. Raman wavenumbers used to conduct PCA labelled in Fig. 2.

total of 95.59 % of the variation in Raman spectra between the two sample types (Fig. 3). The One-way PERMANOVA revealed that this difference was statistically significant between the resilin-rich and chitinous samples (F = 27.39, Bonferroni-corrected P < 0.001).

Assessing the PC variance reveals that peaks at 485–567 cm⁻¹, 955–962 cm⁻¹, 1141–1203 cm⁻¹, and 1615 cm⁻¹ explain most of the differences between the semilunar process and the hind femur control region (Fig. 3). The clustering can be explained not only by the presence of resilin-rich areas but also by vibration changes in the structure of the biomolecule due to binding to different biological structures, such as chitin.

4. Discussion

Our study demonstrates that Raman spectroscopy is a potentially powerful tool for assessing the relative abundance, composition, and distribution of resilin in insect cuticles. The main peaks we identified which likely correspond to the components of resilin include two bands associated with tyrosine at 955–962 and $1141-1203 \text{ cm}^{-1}$ [14,17], and a strong peak at 1615 cm⁻¹ which is attributed to the amide I group associated with dityrosine. The latter offers particularly strong confidence in the presented methodology due to the similarities of its scattering wavenumber with that observed in the synthetic proresilin AN16 [14,17,18]. Although the insect cuticle is rich with other tyrosine-based proteins, the signal associated with tyrosine at 1141–1203 cm⁻¹ was much smaller than in the semilunar process (Fig. 2). This may indicate that this peak is better attributed to dityrosine, which is abundant in the semilunar process [3–5]. The intensity of different peaks will depend on the relative abundance of different proteins within the sample, and our efforts to obtain spectra for the highly fluorescent dityrosine may reduce our ability to discern co-occurring smaller peaks with high resolution.

Our assessments of the structure of insect cuticle match the spectra observed in early studies of the locust cuticle using microtomy and Raman [6]. Although invasive, this early study demonstrated the spatial resolution that can be achieved in insect tissues using Raman, and here we support the findings can be repeated in situ. An important point to highlight is the fact that the Raman signal changes with high level of dehydration of the sample as it is well-known that protein structure changes with differences in solvation and modification of its chemical environment. As Raman is an excellent tool for structural characterization, this highlights the importance of in situ non-invasive analysis to achieve realistic observations of these elastic proteins in their native biological environment and explains the ability of this technique to identify binding to different biological structures, as demonstrated by our experiments.

PC analysis revealed that the aforementioned peaks associated with tyrosine and dityrosine, as well as the chitin skeletal modes at 485–567 $\,\mathrm{cm}^{-1}$, explain most of the variation between the spectra of the two regions of the leg, and should be important for developing this method into the future. We recommend long exposure times at low laser intensities as a main method to reduce fluorescence.

Despite multiple attempts, collection of Raman spectra for the synthetic L,L-dityrosine was not possible using the presented method, with spectra becoming saturated by a high degree of autofluorescence, which is detrimental to Raman analysis. While methods such as surfaceenhanced Raman spectroscopy (SERS) could be used to reduce or completely eliminate fluorescence [19], this would result in shifts to the peaks within the spectra and their ratios, and require invasive nanoparticle delivery, defeating the objective of advancing Raman into noninvasive studies of insect tissues, although a future description of this synthetic dityrosine could be beneficial for generally understanding the mechanism behind dityrosine fluorescence. Dityrosine had significantly greater autofluorescence across all available filter sets, suggesting a broadband autofluorescence (Supplemental Fig. 2). This synthetic dityrosine was also highly instable, changing in response to the temperature of the experimental area (Supplemental Fig. 3), making further

manipulations challenging. This behavior of the isolated dimer, and the fact resilin presents a good in situ Raman signal, highlights the importance of maintaining the native chemical environment in the analysis of proteins in order to understand biological function and maintain structural integrity, as achieved by our Raman observations.

Despite challenges collecting spectra on the highly fluorescent samples, Raman offers a powerful and complimentary method to traditional resilin imaging. While fluorescence can be used to identify resilin-rich tissues [5], Raman can be utilized for in situ descriptions of the native structure. Where resilin and its binding to other tissues vary, the spectra obtained through this methodology will change.

From here, it would be beneficial to investigate the potential for using Raman in a semi-quantitative manner to measure the abundance of resilin/dityrosine in different insect tissues. A sensible model for such an investigation would be the locust wing hinge, which is known to contain about 25 % of its tyrosine in the form of the dimer dityrosine [2,20]. Furthermore, well studied resilin-rich structures such as the pleural arches of froghoppers [21], wing tendons of the dragonfly [2,22], and the metathorax of the flea [23-25], will be useful for advancing such studies in a comparative framework, and could aid in describing the different ways in which resilin is deposited in insect tissues during development. Across species, the method could also be used to address the question of whether resilins utilized for different functions (e.g. flying, jumping) show different structural compositions. In insects where the exterior cuticle is sufficiently transparent or translucent, this method could be tailored to allow us to record protein compositions and structures in live insects thanks to its confocal nature (Supplemental Fig. 1), with uses such as non-invasive dietary analysis, and measurements of internal tissues and hearing organs [26]. Dynamic measurements using Raman could also provide tracking of insect proteins such as resilin through rapid in situ data acquisition to track secondary and tertiary conformational changes to protein structures during function. This could be particularly beneficial in understanding the higher-level vibrational modes of resilin, and differential folding of resilins across different parts of the insect body. Future efforts should seek to develop this methodology alongside traditional methods to build a library of resilin structures across insect structures and taxa, to better understand the diversity of resilin and its native forms.

5. Conclusions

Through the use of non-invasive Raman spectroscopy, we confirm that differentiation of integrated insect proteins is possible with a high resolution. We describe, for the first time, the structural differences in resilin-rich and resilin-poor insect tissues using confocal Raman, demonstrating reliable assignment of peaks within the spectra, and offer a library of such peaks for future research. The main peaks of resilin include two bands associated with tyrosine at 955-962 and 1141-1203 cm^{-1} and a strong peak at 1615 $\text{cm}^{-1},$ attributed to the $\alpha\text{-Amide I}$ group associated with dityrosine. We also found the chitin skeletal modes at ~485–567 cm⁻¹ to be significant contributors to spectra variance between the groups. We suggest Raman to be a complimentary noninvasive method to traditional fluorescence imaging to confirm the presence of resilin in insect tissues without losing structural integrity and its ability to establish binding to different biological structures. Another benefit of Raman is that it can be utilized for in situ descriptions of the native structure without altering the original structure, as dehydration of the protein will imply change in conformation. This is especially useful when observing live specimens. The confocal nature of Raman helps identifying layers of protein, which is not possible with fluorescence. On the negative side, the analysis of resilin using Raman presents a high degree of autofluorescence, which is detrimental. This was partially solved using PCA to identify different resilin regions within the anatomy of the insect.

Statement of significance

We believe this study will be of interest to your readers as it describes the first report of the use of Raman spectroscopy for the identification of the elastic protein resilin inside insect structures in a non-invasive way. Resilin is a very interesting biopolymer and an elastic protein with a high elastic coefficient. It has attracted interest from several companies aiming to the exploit its elastic properties.

The work developed here is an example of the use of Raman spectroscopy in the study of biomolecules and biomaterials for non-invasive, in situ analysis in insects. It also opens the door to understanding their biological function by potentially following conformational changes of proteins in living organisms using Raman spectroscopy.

Declaration of competing interest

The authors declare that they have no known competing financial interests or personal relationships that could have appeared to influence the work reported in this paper.

Acknowledgements

We thank Prof. Malcolm Burrows for the use of his DAPI-equipped microscope. CW's PhD studentship is funded by the University of Lincoln's School of Life and Environmental Sciences. This study was funded by a European Research Council Grant ERCCoG-2017-773067 (to FMZ for the project "The Insect Cochlea") and an NSF-NERC grant NSF DEB-1937815 - NE/T014806/1 (to FMZ).

Appendix A. Supplementary data

Supplementary data to this article can be found online at https://doi.org/10.1016/j.jibiomac.2023.127967.

References

- [1] T. Weis-Fogh, A rubber-like protein in insect cuticle, J. Exp. Biol. 37 (1960) 889–907. https://doi.org/10.1242/jeb.37.4.889
- [2] C.M. Elvin, A.G. Carr, M.G. Huson, J.M. Maxwell, R.D. Pearson, T. Vuocolo, N. E. Liyou, D.C.C. Wong, D.J. Merritt, N.E. Dixon, Synthesis and properties of crosslinked recombinant pro-resilin, Nature 437 (2005) 999–1002, https://doi.org/10.1038/nature04085.
- [3] S.O. Andersen, Characterisation of a new type of cross-linkage in resilin, a rubber-like protein, Biochim. Biophys. Acta 69 249–262 (n.d.).
- [4] S.O. Andersen, T. Weis-Fogh, Resilin. A rubberlike protein in arthropod cuticle, Adv. Insect Phys. 2 (1964) 1–65, https://doi.org/10.1016/S0065-2806(08)60071-
- [5] M. Burrows, G.P. Sutton, Locusts use a composite of resilin and hard cuticle as an energy store for jumping and kicking, J. Exp. Biol. 215 (2012) 3501–3512, https:// doi.org/10.1242/jeb.071993.
- [6] M. Truchet, B. Mauchamp, Characterization of the insect cuticle layers by laser Raman spectrometry, Chitin Nat. Technol. (1986) 13–19, https://doi.org/10.1007/ 978-1-4613-2167-5 3.
- [7] H.J. Butler, L. Ashton, B. Bird, G. Cinque, K. Curtis, J. Dorney, K. Esmonde-White, N.J. Fullwood, B. Gardner, P.L. Martin-Hirsch, M.J. Walsh, M.R. McAinsh, N. Stone, F.L. Martin, Using Raman spectroscopy to characterize biological materials, Nat. Protoc. 11 (2016) 664–687, https://doi.org/10.1038/ nprot.2016.036.
- [8] P.F. McMillian, A. Hofmeister, Infrared and Raman spectroscopy, in: F. C. Hawthorne (Ed.), Spectrosc. Methods Mineral. Geol, Mineralogical Society of America, Washington, DC, 1988, pp. 99–159.
- [9] G. Giridhar, R.R.K.N. Manepalli, G. Apparao, Confocal Raman Spectroscopy, Elsevier Inc., 2017, https://doi.org/10.1016/B978-0-323-46140-5.00007-8.
- [10] Ø. Hammer, A.T.D. Harper, P.D. Ryan, Past: paleontological statistics software package for education and data analysis, Palaeontol. Electron. 4 (2001).
- [11] M. Burrows, Development and deposition of resilin in energy stores for locust jumping, J. Exp. Biol. 219 (2016) 2449–2457, https://doi.org/10.1242/ jeb.138941.
- [12] V.A. Iconomidou, G.D. Chryssikos, V. Gionis, J.H. Willis, S.J. Hamodrakas, "Soft"-cuticle protein secondary structure as revealed by FT-Raman, ATR FT-IR and CD spectroscopy, Insect Biochem. Mol. Biol. 31 (2001) 877–885.
- [13] C.Y. She, N.D. Dinh, T.T. Anthony, Laser Raman scattering of glucosamine, nacetylglucosamine, and glucuronic acid, Biochem. Biophys. Acta 372 (1974) 345–357.

- [14] E. Degtyar, B. Mlynarczyk, P. Fratzl, M.J. Harrington, Recombinant engineering of reversible cross-links into a resilient biopolymer, Polymer (Guildf.) 69 (2015) 255–263
- [15] A. Bertoluzza, C. Fagnano, C. Caramazza, E. Barbaresi, S. Mancini, In vivo Raman spectroscopy of human, animal and artificial ocular lenses, J. Mol. Struct. 214 (1989) 111–117, https://doi.org/10.1016/0022-2860(89)80008-0.
- [16] S.J. Hamodrakas, S.A. Asher, G.D. Mazur, J.C. Reiger, F.C. Kafatos, Laser raman studies of protein conformation in the silkmoth chorion, Biochim. Biophys. Acta 703 (1982) 216–222.
- [17] S.J. Hamodrakas, E.I. Kamistos, A. Papanikolaou, Laser-raman spectroscopic studies of the eggshell (chorion) of Bombyx mori, Int. J. Biol. Macromol. 6 (1984) 333–336
- [18] K.M. Nairn, R.E. Lyons, R.J. Mulder, S.T. Mudie, D.J. Cookson, E. Lesieur, M. Kim, D. Lau, F.H. Scholes, C.M. Elvin, A synthetic resilin is largely unstructured, Biophys. J. 95 (2008) 3358–3365.
- [19] A. Szaniawska, A. Kudelski, Applications of surface-enhanced Raman scattering in biochemical and medical analysis, Front. Chem. 9 (2021) 1–7, https://doi.org/ 10.3389/fchem.2021.664134.
- [20] S.O. Andersen, Covalent cross-links in a structural protein, resilin, Acta Physiol. Scand. Suppl. 263 (1966) 1–81.

- [21] M. Burrows, S.R. Shaw, G.P. Sutton, Resilin and chitinous cuticle form a composite structure for energy storage in jumping by froghopper insects, BMC Biol. 6 (2008) 1–16, https://doi.org/10.1186/1741-7007-6-41.
- [22] S.N. Gorb, Serial elastic elements in the damselfly wing: mobile vein joints contain resilin, Naturwissenschaften 86 (1999) 552–555, https://doi.org/10.1007/ s001140050674.
- [23] M. Rothschild, J. Schlein, The jumping mechanism of Xenopsylla cheopis I. Exoskeletal structures and musculature, Philos. Trans R. Soc. B. 271 (1975) 457–490. http://rstb.royalsocietypublishing.org/content/315/1174/305.abstract.
- [24] M. Rothschild, J. Schlein, K. Parker, C. Neville, S. Sternberg, The jumping mechanism of Xenopsylla cheopsis III. Execution of the jump and activity, Philos. Trans R. Soc. B. 271 (1975) 499–515. http://rstb.royalsocietypublishing.org/content/315/1174/305.abstract.
- [25] G.P. Sutton, M. Burrows, Biomechanics of jumping in the flea, J. Exp. Biol. 214 (2011) 836–847, https://doi.org/10.1242/jeb.052399.
- [26] F.A. Sarria-S, B.D. Chivers, C.D. Soulsbury, F. Montealegre-Z, Non-invasive biophysical measurement of travelling waves in the insect inner ear, R. Soc. Open Sci. 4 (2017) 1–11, https://doi.org/10.1098/rsos.170171.